Stress Evolution During Nanoindentation in Open TSVs

Santo Papaleo, Wolfhard H. Zisser, Anderson P. Singulani, Hajdin Ceric, and Siegfried Selberherr, *Fellow, IEEE*

***Abstract*—We applied a nanoindentation technique in an open through silicon via structure by means of simulations. During nanoindentation, a spherical diamond indenter penetrates into the device by applying a force. This penetration causes displacement and deformation of the materials. The simulation results were compared with experimental data, as loading force versus penetration depth. Consequently, we estimated the areas in the structure, in which a mechanical failure due to an external load can be expected. Our simulations revealed the regions with the highest concentration of mechanical stress. These are the critical areas in which the probability of device failure, such as cracking or delamination, is at its highest.**

***Index Terms*—Nanoindentation, TSV.**

I. Introduction

THREE-DIMENSIONAL technology is considered a necessity for ensuring that integrated circuit performance continues along the path described by Moore's law. Such technologies would be a boon to semiconductor device development by facilitating increased system functionality and integration density [1], [2].

Through Silicon Vias (TSVs) are interconnections used for 2.5D and 3D integrated circuit technologies. The TSV fabrication process consists of filling a hole using a metal material. Two different approaches are possible: filled or unfilled (open) TSVs. Due to the different thermal expansion between constituent materials, fabrication of the TSV induces thermal stress, thereby possibly degrading the performance of the device. Of the two approaches, the unfilled configuration is therefore favored. The unfilled configuration allows the filling material to expand towards the center of the TSV limiting critical stress in the structure [1].

In this work we studied the evolution of stress during nanoindenation in an open TSV (see Fig. 1). Usually, nanoindentation is employed to evaluate the elastic modulus, strain-hardening exponent, fracture toughness, and the viscoelastic properties. In our study nanoindentation was used to reproduce an external load acting on an open TSV. This external load can represent extra mechanical stress during the fabrication processes (for example, as occurs during bonding between dies or between interposer layer and die [2]), or an accidental load, for example due to particles. The main goal of this work was to estimate the areas in which mechanical failure due to an external load can be expected. From the results, a better understanding of how to increase the mechanical stability of the system can be gleaned.

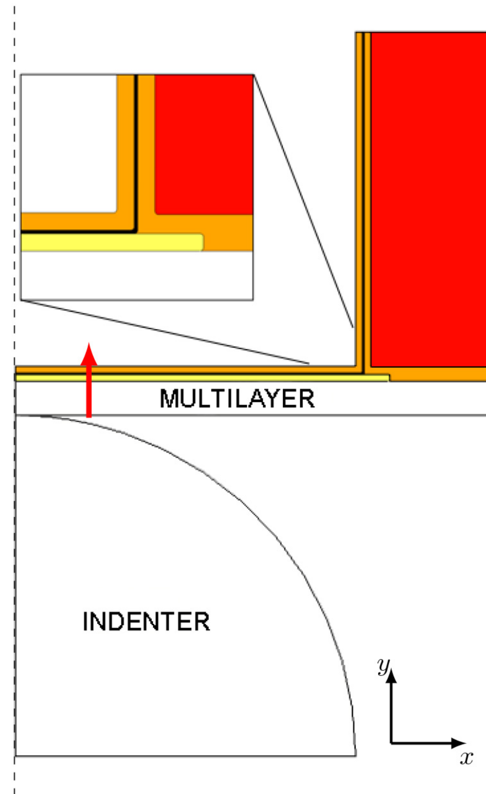

Fig. 1. Two-dimensional representation of a TSV structure and indenter. The dashed line indicates the axis of symmetry. Only a quarter of the system is represented. Al is shown in yellow, W in black, SiO_2 in orange, and Si in red. The multilayer consists of different materials. The indenter is spatially external to the TSV (the via height and width of the TSV in the figure do not represent the real size, under consideration).

The mechanical reliability of TSVs is strongly connected to the material properties and the size of the device. Materials behave differently under mechanical stress and can therefore affect the mechanical stability of the system. The bottom portion of an open TSV can be composed of

Manuscript received August 30, 2016; accepted October 25, 2016. Date of publication October 28, 2016; date of current version December 2, 2016.

S. Papaleo and H. Ceric are with the Christian Doppler Laboratory for Reliability Issues in Microelectronics at the Institute for Microelectronics, TU Wien, 1040 Wien, Austria (e-mail: papaleo@iue.tuwien.ac.at; ceric@iue.tuwien.ac.at).

W. H. Zisser and S. Selberherr are with the Institute for Microelectronics, TU Wien, 1040 Wien, Austria (e-mail: zisser@iue.tuwien.ac.at; selberherr@iue.tuwien.ac.at).

A. P. Singulani is with ams AG, 8141 Unterpremstaetten, Austria (e-mail: anderson.pires_singulani@ams.com).

Color versions of one or more of the figures in this paper are available online at http://ieeexplore.ieee.org.

Digital Object Identifier 10.1109/TDMR.2016.2622727

1530-4388 © 2016 IEEE. Personal use is permitted, but republication/redistribution requires IEEE permission.
See http://www.ieee.org/publications_standards/publications/rights/index.html for more information.

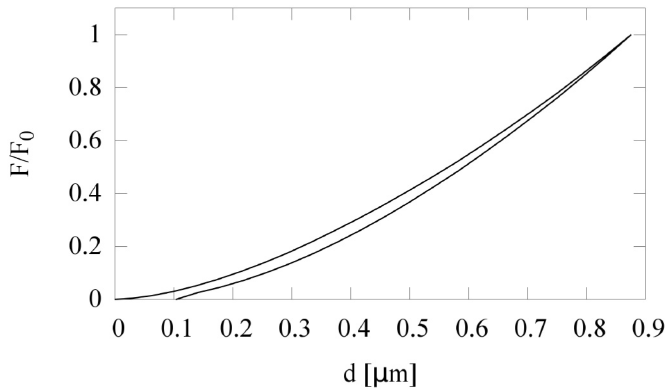

Fig. 2. An example of a load-displacement curve (normalized force versus displacement into surface).

different material layers. During the deposition processes and fabrication steps (die bonding, etc.), new mechanical stresses can be generated leading to mechanical instability. Mechanical stresses, in turn, determine the formation of new defects or the propagation of existing defects in the structure. The material properties and device geometry must therefore be optimized in order to minimize mechanical stresses and to improve reliability [3].

We have therefore analyzed nanoindentation by means of the finite element method (FEM) [4] and we compared the simulation results with experimental data. The information obtained contributes to a better understanding of the mechanical stability of TSV technology.

II. Nanoindentation

Nanoindentation is a simple method which consists of touching the material of interest with another material. In one of these two materials, the mechanical properties, such as elastic modulus and hardness, are unknown. In the other, the material properties are known.

During nanoindentation, an indenter is placed in contact with the surface of a sample in which a steadily increasing load is applied. This causes the indenter to penetrate into the sample. Indenters can be adapted to suit the parameters under investigation and can therefore have different shapes and can be composed of different materials. Indenters are identified as spherical, conical, Vickers, and Berkovich [5]. The applied force at the indenter is usually in the millinewton range, and the depth of penetration is on the order of micrometers.

Very important results of nanoindentation are load-displacement curves. Both load and depth of penetration are recorded at each load increment. Following the measurement of the maximum load, the load is steadily removed, and the penetration depth is recorded again. If a residual impression is left on the surface of the specimen, a plastic deformation in the material has occurred. In contradistinction, if the removal of the indenter does not leave an impression, the material has behaved elastically.

Fig. 2 depicts an example of a load-displacement curve. The top line represents the loading while the indenter is penetrating the sample. The bottom line, on the other hand, depicts the unloading during which the indenter is extracted from the sample. In this example, the sample plastically deforms. The plastic response is detectable because the unloading curve does not return to its initial displacement value. A residual impression due to plastic deformation of the material therefore remains. Usually, the loading portion of the indentation cycle consists of an elastic response of the material at lower loads followed by plastic flow, or yield, within the sample at higher loads [5].

III. Analyzed System

FEM was used to simulate the nanoindentation technique as applied to an open TSV. From the simulation results, information regarding the development of mechanical stress in the device is obtained.

In these simulations the bottom part of the open TSV is mechanically fixed laterally at the Si sidewall. The bottom area is thereby "free" to bend in the y-axis (red arrow in Fig. 1). This structure corresponds to the step before die bonding, and it corresponds to a structure used for optical sensor applications [1], [6]. During the process of fabrication, a critical mechanical stress can be generated. High concentrations of mechanical stress can cause failure in the form of cracking and delamination in the layers which compose the bottom of the TSV.

The bottom of the TSV under consideration consists of a multilayer structure which corresponds to the Al based interconnection structure for CMOS technology [1]. These layers are materials with different thicknesses and mechanical properties. In the following, this many-layered structure is diagrammatically depicted as a single layer, denoted as "multilayer" in Fig. 1. The mechanical and electromechanical properties of the materials play an important role regarding the reliability of devices. Mechanical properties of thin films should be accurately measured at the length scale of the devices under consideration, since their properties are different from those of bulk materials. These difference, can be due to size effects, grain structures, and processing [7].

IV. Simulation Setup

In an open TSV, the indenter can be placed in two different locations, either internal or external to the TSV. These two locations will produce a different distribution of mechanical stress in the TSV. In this work, an indenter acting external to an open TSV, as shown in Fig. 1, was considered. A spherical diamond indenter with a radius of 50 μm, a Young's modulus of 1100 GPa, and a Poisson's ratio of 0.07 were used. The TSV aspect ratio is 1:2.5 and the TSV diameter is 100 μm [1]. The layers have thicknesses of 1 μm for SiO_2, 1 μm for the Al layer, and 0.2 μm for W.

The simulations were performed by accounting for each material of the multilayer, rather than considering just a single artificial one (Fig. 1). A two-dimensional axisymmetric simulation setup was performed. The materials used in an open TSV have a polycrystalline or amorphous structure. An isotropic behavior can therefore be assumed. This setting leads

to a simplification of the simulation. Because of the location of the indenter, the mechanical stress is mainly generated at the multilayer area and not at the Si in the sidewall. We therefore assumed that Si does not significantly influence the mechanical stability of the multilayer, and hence it was assumed to be isotropic. Only a negligible influence of the anisotropy of the Si on the final results is expected.

To reproduce the process of nanoindentation, the FEM simulation requires a contact condition between indenter and sample to recreate the interaction between TSV bottom and indenter during penetration. In the implemented model, this condition was reproduced by employing the contact pressure penalty method [4], [5].

Accurate results are obtainable by modeling the contact areas of the indenter and the membrane with a very fine FEM mesh. In general, all geometries would benefit from a fine mesh, but this would lead to excessively long simulation times. A fine mesh was therefore used at the contact area of the indenter and the sample only. A mapped mesh with a mesh size of 0.5 μm was employed for the layer in contact with the indenter. For the indenter, a triangular mesh was employed. Along the edge of the indenter in contact with the TSV, a maximum mesh size of 0.06 μm was used.

A stationary parametric sweep study was performed. The movement of the indenter was emulated by using the prescribed displacement as variable. This was repeated for increasing displacements, until the maximum measured displacement from the experimental data was reached.

The TSV structure was mechanically fixed at the top of the TSV sidewall. For the outer-rightmost Si region, a so-called roller constraint was chosen, which allows the material to move perpendicular to the boundary but not normal to it. On the other edges, the TSV was free to move, allowing for a reproduction of the real conditions of the device.

V. Plasticity Simulation

In the implemented model, the elastic-plastic behavior of the materials was considered. The elastic behavior was reproduced with Hooke's law. The plastic behavior was described by employing an isotropic hardening law [4], [8].

An elastic-plastic material is usually modeled under the assumption that the strains (ε) and strain increments ($d\varepsilon$) formed by the elastic and plastic part can simply be added.

$$\varepsilon = \varepsilon_e + \varepsilon_p, \qquad d\varepsilon = d\varepsilon_e + d\varepsilon_p \tag{1}$$

By coupling the elastic part, described by Hooke's law, and the plastic part in (1), the stress σ in a material is described as

$$\sigma = C : \varepsilon_e = C : \left(\varepsilon - \varepsilon_p\right), \tag{2}$$

where C is the elasticity tensor.

When considering an isotropic plastic material, the strain increment is studied by using the plastic potential Q_p, which is a function of the three invariants of Cauchy's tensor

$$Q_p(\sigma) = Q_p(I_1(\sigma), J_2(\sigma), J_3(\sigma)), \tag{3}$$

where the three invariants are defined by

$$\begin{aligned} I_1 &= \sigma_{11} + \sigma_{22} + \sigma_{33}, \\ J_2 &= \frac{1}{2}\left(\sigma_{ii}\sigma_{jj} - \sigma_{ij}\sigma_{ji}\right), \\ J_3 &= \sigma_{11}\sigma_{22}\sigma_{33} + 2\sigma_{12}\sigma_{23}\sigma_{31} - \sigma_{12}^2\sigma_{33} - \sigma_{23}^2\sigma_{11} - \sigma_{31}^2\sigma_{22}. \end{aligned} \tag{4}$$

An increment of the plastic strain tensor $\dot{\varepsilon}_p$ can therefore be decomposed as

$$\dot{\varepsilon}_p = \lambda \frac{\partial Q_p}{\partial \sigma} = \lambda \left(\frac{\partial Q_p}{\partial I_1}\frac{\partial I_1}{\partial \sigma} + \frac{\partial Q_p}{\partial J_2}\frac{\partial J_2}{\partial \sigma} + \frac{\partial Q_p}{\partial J_3}\frac{\partial J_3}{\partial \sigma} \right), \tag{5}$$

where λ is the plastic multiplier, which depends on the current state of the stress and the load history. The "dot" in $\dot{\varepsilon}_p$ does not indicate a true time derivative, but rather it indicates the rate at which the plastic strain tensor changes with respect to $\partial Q_p/\partial\sigma$. The employed measure of the plastic deformation is the effective plastic strain rate $\dot{\varepsilon}_{pe}$, which is defined as

$$\dot{\varepsilon}_{pe} = \sqrt{\frac{2}{3}\dot{\varepsilon}_p : \dot{\varepsilon}_p}. \tag{6}$$

In the theory of plasticity, it is possible to describe yielding only in the terms of σ by means of a yield function. A yield function can therefore be used to define the onset of plastic behavior. The yield function $F_y(\sigma, \sigma_{ys})$ defines the limits of the elastic regimes. For $F_y(\sigma, \sigma_{ys}) < 0$, the material reacts elastically, and for $F_y(\sigma, \sigma_{ys}) \geq 0$, on the other hand, it begins to deform plastically [8].

$\sigma_{ys}(\varepsilon_{pe})$ is the current yield stress which evolves during plastic flow and is described by an isotropic hardening law. The isotropic hardening law under consideration is a linear equation described by

$$\sigma_{ys}\left(\varepsilon_{pe}\right) = \sigma_{ys0} + \frac{E_{Tiso}}{1 - \frac{E_{Tsio}}{E}}\varepsilon_{pe}, \tag{7}$$

where σ_{ys0} is the initial yield stress (a material property), which indicates the stress level at which plastic deformation occurs. As we can see in (7), $\sigma_{ys}(\varepsilon_{pe})$ is determined by the isotropic tangent modulus E_{Tiso} and the effective plastic strain ε_{pe}. The yield level increases proportionally to the effective plastic strain ε_{pe} [4], [8].

The yield function is defined as

$$F_y = \sigma_{mises} - \sigma_{ys}\left(\varepsilon_{pe}\right), \quad Q_p = F_y, \tag{8}$$

where σ_{mises} is the Von Mises stress, though it is possible to define it differently.

Not only do the material parameters influence the load-displacement curves, but nanoindentation is also sensitive to the level of residual stress in the layers. The results of experimental indentation are therefore the sum of two contributions: plastic deformation and residual stress.

VI. Results and Discussion

The model was calibrated using experimental data. Calibration permits an understanding of how mechanical stress develops within the different layers (multilayer) as the force applied by the indenter increases. The experimental data were

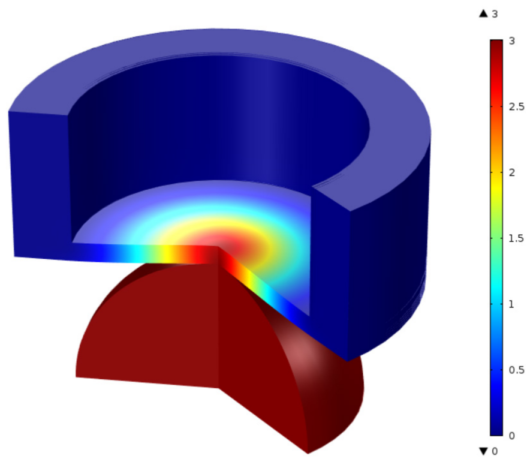

Fig. 3. FEM result. This figure illustrates the displacement of the indenter inside of the TSV. The different colors indicate the displacement in μm.

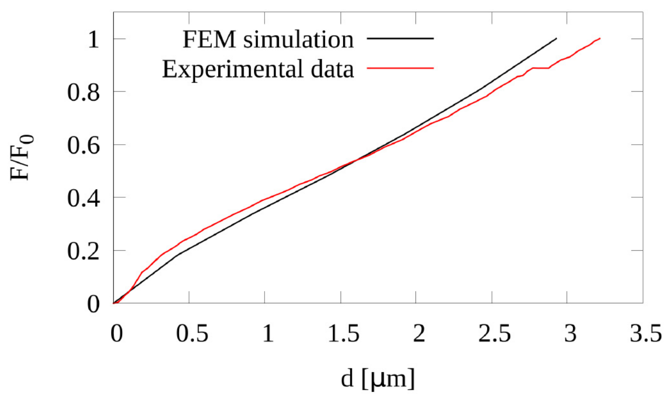

Fig. 4. The loading part of the nanoindentation process is plotted above and illustrates a comparison between the FEM simulation and experimental data.

obtained up to a displacement of the indenter into the surface of approximately 3 μm. During the experiment, the process of unloading was not recorded.

In Fig. 3 the FEM result shows the indenter at the highest prescribed indentation displacement. The movement of the indenter causes it to penetrate approximately 3 μm into the multilayer, which results in the displacement and deformation of the materials. The highest displacement is found at the center of the device. The deformation of the sample develops around the contact point between indenter and sample, and increases as the load is applied.

From the experimental data it was possible to obtain the load-displacement curve. The loading plot provides information about the mechanical properties, as well as the failure of the device. In Fig. 4 the red line indicates the experimental data and the black line, the FEM results. Due to the architecture of TSVs, the experimental results do not represent the behavior of only one material, but rather the behavior of a multilayer structure. In the experimental data shown in Fig. 4 we can identify an initial elastic regime which corresponds to an indentation displacement between 0 to 0.25 μm, followed by a plastic regime for indentation displacements above 0.25 μm. An aberration is observable around an indentation displacement of 2.5 μm and is assumed to be due to a failure in the device, such as cracking or delamination [5].

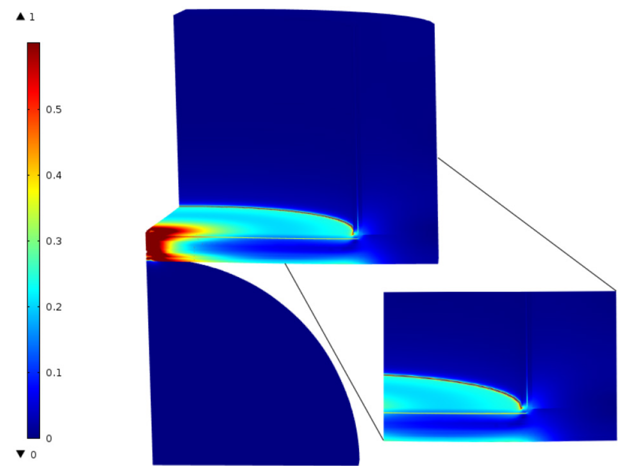

Fig. 5. This image depicts normalized Von Mises stress development in the TSV. Two physical regions with high mechanical stress can be identified. The first is located in the TSV area above the indenter and the second is at the corner of the TSV. This perspective of the structure differs from Fig. 1 in order to highlight those areas with a high concentration of mechanical stress.

The results of the simulation are in good agreement with experimental data, as can be seen in Fig. 4. It is particularly important to have a good fit for low loads of the indenter, in the range of 0 to 0.1 F/F_0, because in this range only the elastic behavior of the materials influences the results. The fitting of the plastic regime requires much more effort, because the bottom of the TSV consists of different materials. Each material could exhibit plasticity, which can occur when different sufficiently high loads are applied. Furthermore, the plastic properties of thin layers employed in TSV structures are not reported in the literature. The plastic response of plastic materials during loading was described with (7), where the yield stress and isotropic tangent modulus are the fitting parameters [9]–[11]. The results of the simulation depend on the values of the yield stress and the isotropic tangent modulus of the materials. To fit the model with the experimental data, we changed: i) the values of the yield stress, and ii) the isotropic tangent modulus of the plastic materials of the multilayer, which were met by the indenter during indentation. By changing these parameters, we found a good match with the experimental data. The deviation between the experimental results and the simulations is due to the multilayer structure for which the composition between layers and the non-bulk character can have an influence on the plastic behavior, which was not taken into account.

During deposition processes, residual stresses develop in the layers of the multilayer structure. Film residual stresses can influence the nanoindentation test [5]. Different values of residual stress [12] were set in thin films of the multilayer. These tests did not improve the fitting, and the residual stress was therefore not considered.

Fig. 5 depicts the normalized Von Mises stress due to nanoindentation in the TSV. Two locations with high mechanical stress can be seen. The first is above the indenter, and the second is located at the bottom corner of the TSV sidewall. The first interaction with the indenter generates a critical mechanical stress only in this area. As the indenter penetrates

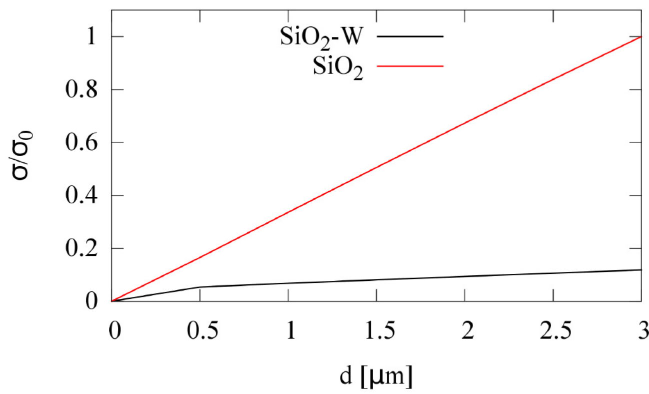

Fig. 6. Normalized Von Mises stress versus displacement into surface.

into the TSV, the mechanical stress develops and becomes problematic at the corner of the TSV sidewall.

An increase in the displacement of the indenter increases the stress in the TSV. The inset in Fig. 5 depicts in detail the distribution of the Von Mises stress in the W layer. High mechanical stress can cause reliability issues. Specifically, it can induce delamination and cracking at the interface. From the simulations we obtained the values of the stress at different locations in order to determine which mode of failure is most likely to occur.

Fig. 6 illustrates the Von Mises stress development at the corner of the TSV sidewall. We compared the highest stress in the SiO_2 at the corner of the TSV with the highest stress at the interface between the SiO_2 and the W layer, close to the corner of the TSV. This figure reveals an increase in stress during the penetration of the indenter into the TSV. This result indicates a continuous increase in stress at the surface of the SiO_2. At the SiO_2-W interface, the stress behaves differently. First, it grows continuously exhibiting a smaller slope than the maximum stress at the surface of the SiO_2. After an indentation of approximately 0.5 μm is reached, the slope is further reduced. This does not indicate that the failure will be confined to the surface of the SiO_2, because the interface could have defects or a small interface fracture toughness, which may result in cracking or delamination, and which can strongly contribute to the failure of the interface.

The simulations can predict the areas of the device in which there is a high probability of failure. We found the following scenario:

- Initially, only the area of the TSV above the indenter appears to be problematic. During indentation, the concentration of stress can increase, until a failure occurs. The presence of defects can facilitate delamination or cracking.
- At higher indentations, the stress becomes an issue at the corners of the TSV. In this area we can expect cracking of the SiO_2. The cracks can then propagate, and when they reach an interface, can cause delamination.

VII. Conclusion

We investigated the stress development in the layers of open TSVs during nanoindentation. The implemented model permits to simulate the penetration of the indenter into the bottom of the TSV, reproducing the extra mechanical stress which might act during the fabrication process. The simulations were matched with experimental data. The model was fitted qualitatively by altering the material parameters of plasticity. Areas of critical stress, located above the indenter and at the corner of the TSV, were identified. Our model can be used to identify the way in which geometric and material properties influence the mechanical stability of TSVs.

References

[1] J. Kraft *et al.*, “3D sensor application with open through silicon via technology,” in *Proc. ECTC*, Lake Buena Vista, FL, USA, 2011, pp. 560–566.
[2] P. E. Garrou, C. A. Bower, and P. Ramm, *Handbook of 3D Integration*, vol. 1. Weinheim, Germany: Wiley-VCH-Verlag, 2008.
[3] A. P. Karmarkar, X. Xu, and V. Moroz, “Performance and reliability analysis of 3D-integration structures employing through silicon via (TSV),” in *Proc. IEEE Int. Rel. Phys. Symp.*, Montreal, QC, Canada, 2009, pp. 682–687.
[4] *COMSOL Multiphysics v.5.1.*, COMSOL AB, Stockholm, Sweden.
[5] A. C. Fischer-Cripps, *Nanoindentation* (Mechanical Engineering Series). New York, NY, USA: Springer, 2011.
[6] L. Hofmann *et al.*, “3D integration approaches for MEMS and CMOS sensors based on a Cu through-silicon-via technology and wafer level bonding,” in *Proc. Int. Soc. Opt. Photon. SPIE Microtechnol.*, vol. 9517. Barcelona, Spain, 2015, vol. 9517 pp. 951709–951712.
[7] O. Tabata *et al.*, *Reliability of MEMS: Testing of Materials and Devices* (Advanced Micro & Nanosystems). Weinheim, Germany: Wiley-VCH, 2013.
[8] J. Lubliner, *Plasticity Theory* (Dover Books on Engineering). Mineola, NY, USA: Dover, 2013.
[9] H. D. Espinosa, B. C. Prorok, and M. Fischer, “A methodology for determining mechanical properties of freestanding thin films and MEMS materials,” *J. Mech. Phys. Solids*, vol. 51, no. 1, pp. 47–67, 2003.
[10] H. D. Espinosa, B. C. Prorok, and B. Peng, “Plasticity size effects in free-standing submicron polycrystalline FCC films subjected to pure tension,” *J. Mech. Phys. Solids*, vol. 52, no. 3, pp. 667–689, 2004.
[11] H. Pelletier, J. Krier, A. Cornet, and P. Mille, “Limits of using bilinear stress–strain curve for finite element modeling of nanoindentation response on bulk materials,” *Thin Solid Films*, vol. 379, nos. 1–2, pp. 147–155, 2000.
[12] L. Filipovic, A. P. Singulani, F. Roger, S. Carniello, and S. Selberherr, “Intrinsic stress analysis of tungsten-lined open TSVs,” *Microelectron. Rel.*, vol. 55, nos. 9–10, pp. 1843–1848, 2015.

Santo Papaleo, photograph and biography not available at the time of publication.

Wolfhard H. Zisser, photograph and biography not available at the time of publication.

Anderson P. Singulani, photograph and biography not available at the time of publication.

Hajdin Ceric, photograph and biography not available at the time of publication.

Siegfried Selberherr, photograph and biography not available at the time of publication.